ChemComm

COMMUNICATION

View Article Online
View Journal | View Issue

Cite this: *Chem. Commun.*, 2021, **57**, 5526

Received 12th April 2021,
Accepted 4th May 2021

DOI: 10.1039/d1cc01944a

rsc.li/chemcomm

Fluorescent probe for early mitochondrial voltage dynamics†

Cinthia Hernández-Juárez, Ricardo Flores-Cruz and Arturo Jiménez-Sánchez *

Mitochondrial voltage dynamics plays a crucial role in cell healthy and disease. Here, a new fluorescent probe to monitor mitochondrial early voltage variations is described. The slowly permeant probe is retained in mitochondria during measurements to avoid interferences from natural membrane potential by incorporating an hydrolizable ester function. Voltage, local polarity, pH parameters and transmembrane dynamics were found to be deeply correlated opening a approach in mitochondrial sensing.

Mitochondrial membrane potential ($\Delta\Psi_m$) is now recognized as a universal indicator of mitochondrial function in health and disease.[1] $\Delta\Psi_m$ status is crucial for normal cell growth and differentiation, its disruption however, is directly associated to all types of mitochondrial-related diseases such as cancer, diabetes mellitus, cardiovascular and neurodegenerative disorders, to mention some of them.[2–4] This membrane potential (or voltage) is mainly a consequence of the ionic gradients between the mitochondrial membrane and cytosol,[5] and the proper monitoring of early voltage variations is highly important for the understanding of the molecular basis that govern cell processes in mitochondrial disfunction. However, although several methods have been developed to quantify $\Delta\Psi_m$, most of them are necessarily of the Nernstian behaviour where cationic-lipophilic dyes accumulate in the organelle through the electrochemical gradient (mitochondria has a $\Delta\Psi_m$ *ca.* −180 mV at pH about 8), then several analytical interferences arise as a consequence of dye concentration uptake variations due to mitochondrial depolarization (less negative potential) and hyperpolarization (more negative potential). Another key requirement for $\Delta\Psi_m$ monitoring is that potential variations should be calibrated *vs.* a fluorescence process directly related to the photophysical mechanism giving the voltage response, commonly, intramolecular electron transfer (which is voltage sensitive) is coupled with a proton transfer process.

We hypothesized that, by designing a probe that features a local polarity correlation with $\Delta\Psi_m$ could allow a self-referenced monitoring of the mitochondrial voltage variations with local polarity through the calibrated fluorescence profile of the probe, where such profile can easily be controlled by a photoinduced electron transfer (PET) process inherent of this family of molecular polarity probes.[6,7]

In this work we describe the first molecular probe, called **RVolt**, to monitor early mitochondrial voltage variations through a polarity-referenced and non-releasable mechanism, Fig. 1.

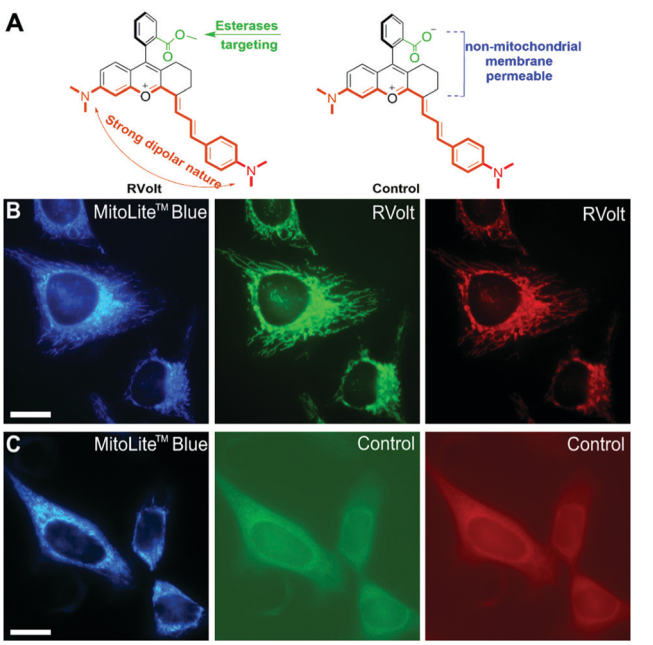

Fig. 1 (A) Chemical structure of the **RVolt** and **Control** probes. Co-localization imaging in live HeLa cells under the using MitoLite™ Blue (blue panels, λ_{exc} = 344 nm, λ_{em} = 469 nm) indicating that (B) **RVolt** is mitochondria-specific with Pearson's coefficient of 0.94 and (C) **Control** is a non-permeable exogenous probe. Scale bars represent 20 μm.

Instituto de Química, Universidad Nacional Autónoma de México, Ciudad Universitaria, Circuito Exterior s/n, De. Coyoacán 04510, Ciudad de México, Mexico. E-mail: arturo.jimenez@iquimica.unam.mx

† Electronic supplementary information (ESI) available. See DOI: 10.1039/d1cc01944a

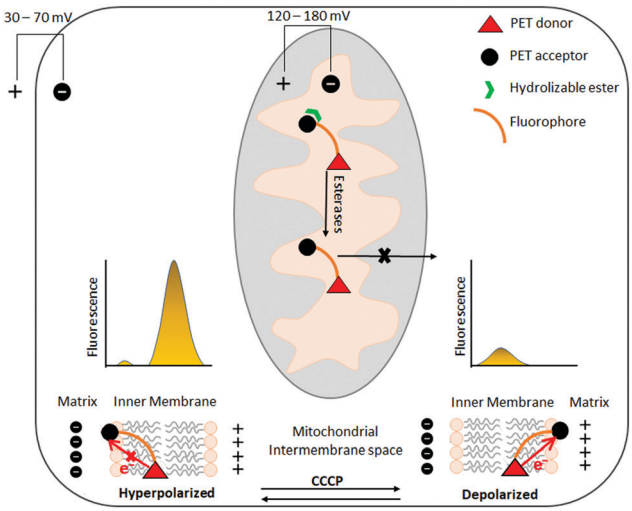

Scheme 1 Sensing mechanism of **RVolt** to monitor early mitochondrial membrane voltage. The probe is internalized and retained in mitochondria through esterase hydrolysis losing its Nernstian features. Then, the PET process is not active in the hyperpolarized membrane which gives more fluorescence, depolarization activates PET and quench the NIR fluorescence. This can be achieved by using carbonyl cyanide 3-chlorophenylhydrazone (CCCP) type uncouplers.

This implies that after loading cells with the Nernstian fluorophore **RVolt** having an acetyl function, mitochondrial membrane is permeabilized. Once the probe is accumulated in the mitochondrial matrix, esterase enzymes could hydrolyze the acetyl ester function,[8] disbalancing the formal charge of the probe and thus trapping **RVolt** between the mitochondrial matrix and the inner membrane. Consequently, the hydrolyzed probe is no longer permeable to the membrane, similar to the slow-equilibrating mitochondrial marker Rhodamine 123,[9] Scheme 1. In fact, **RVolt** is similar to Rhodamine 123 having slowly permeant features,[10] and larger periods of mitochondrial retention, thus allowing almost 1 hour before leaving the mitochondrial outer membrane. Importantly, as **RVolt** is highly dependent on the local polarity, its fluorescent profile calibration towards this physicochemical observable allowed us to have an internal reference to monitor mitochondrial voltage in live cells under conditions promoting membrane potential variations, swelling, permeability transition pore (mPTP) opening and under pH and redox variation controls.

RVolt was synthetized and characterized as described in the ESI.† Then, photophysical properties and high-resolution confocal microscopy studies in HeLa and SK-Lu-1 cells were carried out. The chemical structures and subcellular localization of **RVolt** and an RVolt-derived control, named **Control**, are presented in Fig. 1A. Specific mitochondrial localization was corroborated by co-localization analysis for **RVolt** using the commercial blue-emitter MitoLite™ marker, Fig. 1B. A highly similar co-localization pattern was also found in HK-Lu-1 cells, Fig. S1 (ESI†). Yet normal incubation (exogenous addition) of **Control** molecule to the cells does not lead to a high cell permeabilization and mitochondrial staining. This can be explained by the presence of a free carboxylate function that neutralizes the oxonium-positive charge of the fluorophore and simultaneously directs **Control** mostly to the plasma membrane. Also, while **RVolt** has a partition coefficient $\log P$ = 1.02 (and positively charged), **Control** has a $\log P$ = 0.31 (and neutral, pK_a = 6.78 for the carboxylic deprotonation equilibrium, see ESI†) which is still a bit lipophilic due to the large cinnamic fragment tether to the rhodamine-type structure.

To corroborate the PET process, present in the **RVolt**, a robust photophysical analysis was carried out by means of UV-Vis and fluorescence spectroscopies as well as computational studies.

The computational analysis through a three-model scheme of electron density difference,[11] natural transition orbital (NTO) hole-electron distributions[12] and charge transfer extent index upon photoexcitation[11] for the **RVolt** indicated efficient charge transfer features, Fig. S2 (ESI†). Charge-transfer (CT) indexes upon photoexcitation and NTO eigenvalues are summarized in Fig. S2 and Table S1 (ESI†). Inspection of NTO through the HONTO–LUNTO pairs corroborated a dipolar charge transfer redistribution for both probes. Such solvent polarity and proticity dependence on the fluorescence properties is traduced in a dual-emission band pattern that allowed us to calibrate the probe by using the λ-ratiometric principle, Fig. 2.

As organic solvents can exert a strong influence on the probe photophysics by different empirical parameters (*i.e.*, solvent polarity, polarizability, acidity, basicity and viscosity) at the same time, proper calibration should be conducted in a more controlled media, trying to isolate the effect of dielectric constant as much as possible. Then, as dioxane and water have similar dispersion properties but highly different dipolarities, we implemented a dioxane:H_2O fluorescence titration, Fig. 2, although the solvatochromic analysis in different solvents for **RVolt** is also presented in Table S2 (ESI†). In addition to the dioxane:H_2O continuous variation, we implemented a carbonyl cyanide 3-chlorophenylhydrazone (CCCP) titration in 5 mM HTAB micellar medium in order to calibrate both effects. For both, dioxane:H_2O and CCCP, protonation plays the strongest effect where CCCP promotes a ratiometric change of the Vis and NIR-emission bands corroborating the PET process inhibition, overall less fluorescence emission detected at the NIR band due to the protonation of the dimethylamino(cinnamic)

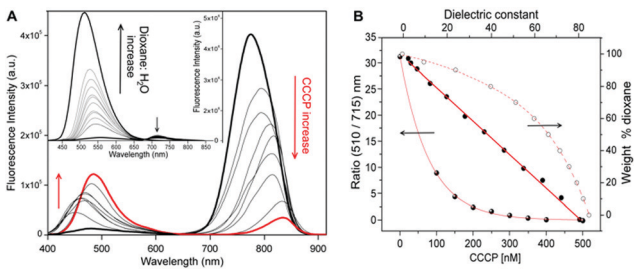

Fig. 2 CCCP and polarity model parameters. (A) Fluorescence spectra (λ_{exc} = 400 nm) of 40 μM **RVolt** at variable CCCP concentration. Inset shows fluorescence spectra of **RVolt** at different dioxane:H_2O v/v mixtures. (B) Ratiometric calibration plot for fluorescence intensity ratio r = 510/715 nm (straight line, middle) at the corresponding CCCP [nM] (filled circles, left) and correlation with % dioxane v/v (hollow circles, right).

moiety. The dioxane:H_2O variation introduces a ratiometric pattern although a stronger activation at the Vis emission band was observed. Then, the ratiometric calibration plot for r = 510/715 nm at the corresponding CCCP [nM] and corresponding % dioxane v/v variation is presented in Fig. 2B. Such calibration provides an excellent tool to correlate the proticity effect coming from the CCCP uncoupler and other protonation effects that can occur in the subcellular environment, *i.e.* osmotically driven water into the membranes. On the other side, high-resolution confocal imaging using an Airyscan detector for HeLa and SK-Lu-1 cells stained with the **RVolt** revealed a clean mitochondrial framework localization. Such filamentous-like morphology was visualized in both, the green (λ_{exc} = 488 nm) and red (λ_{exc} = 647 nm) confocal channel setup during the experiments. Interestingly, confocal imaging studies using CCCP uncoupling agent to depolarize mitochondria demonstrated that once **RVolt** is internalized in the organelle, the mitochondrial localization persisted, although with variable fluorescence intensity from low-dose experiments to high concentration of CCCP (150 nM to 500 nM), Fig. 3A. In order to demonstrate that **RVolt** follows a non-Nernstian mitochondrial localization mechanism, we conducted three key experiments, to know, (1) the fluorescence titration of **RVolt** at variable CCCP concentration to corroborate the observed fluorescence intensity variation, (2) cell imaging reversibility study using CCCP–oligomycin A stimuli, (3) a mitochondrial permeability transition pore (mPTP) opening study to confirm that the **RVolt** is trapped between the mitochondrial matrix and the inner membrane. During the experiments, we used the commercial TMRM® mitochondrial localizer as control, Fig. 3B, although this dye exhibits self-quenching at high concentrations, thus interfering the interpretation of fluorescence intensity changes.

As mentioned, PET process is the photophysical mechanism that allows the probe to report membrane voltage variations without leaving the mitochondria. As protonophores, CCCP or FCCP agents depolarize the mitochondrial inner membrane thus increasing the PET process[13] and changing the fluorescence intensity profile of **RVolt**, Fig. 2 and 3A. As shown, PET is activated upon CCCP protonophore additions, thus resulting in a decrease in fluorescence intensity. To assess the membrane voltage variation monitoring such fluorescence scenario was calibrated and correlated with the fluorescence imaging in cells by tracking membrane depolarization and hyperpolarization. Another feature of the **RVolt** is that the obtained fluorescence intensities can be directly associated with the intrinsic dipolar nature of the probe. For this reason, the λ-ratiometric profile of **RVolt** *vs.* CCCP has a strong linear dynamic range and sensitivity, Fig. 2B. It is worth mentioning that PET process in this type of donor–acceptor fluorophores is always inherently associated with a charge transfer state, in this sense is crucial for any analytical calibration to consider the extent to which local polarity influence the observed fluorescence profile.

We pursued an interference-free scenario of the **RVolt** under a controlled mitochondrial pH using a previously reported protocol by our group,[14] the effect of the mitochondrial membrane potential variations was analyzed using CCCP and oligomycin A (OA) which increases $\Delta\Psi_m$ by inhibition of ATP synthase, leading to a decrease in the reduced respiratory chain intermediates. Thus, we turned to exploring the influence of pH on mitochondrial membrane voltage reversibility by using a 100 nM nigericin stimuli before the depolarization (with CCCP) and hyperpolarization (with OA) treatments.[15] The mitochondrial pH gradient (ΔpH_m) was substantially abolished since nigericin promotes a K^+/H^+ membrane equilibration making $[K^+]_{in} = [K^+]_{out}$, consequently the proton concentration $[H^+]_{in} = [H^+]_{out}$ and $\Delta pH_m = 0$. Live-cell experiments with the **RVolt** probe were always corrected by this control parameter as a starting point. To note, oligomycin increases mitochondrial pH (less $[H^+]_m$), while CCCP decreases mitochondrial pH (more $[H^+]_m$),[16] Fig. 4. As previous cautionary case studies,[17] it is important to consider that positive charges in the membrane voltage dynamics are not only protonic charges as usually interpreted, but also K^+ and Ca^{2+} charges dumping from mitochondria into the cytosol, for such reason even before

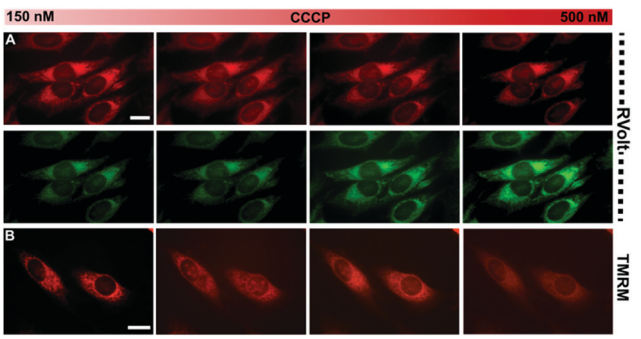

Fig. 3 Time course monitoring of CCCP depolarization changes. (A) Cells are stained with 10 μM **RVolt** and 150 nM CCCP were added. Then, images were recorded after each 5 min with corresponding CCCP additions until reaching 500 nM (λ_{exc} = 488 and 647 nm). (B) TMRM mitochondrial localizer control experiment (λ_{exc} = 605 nm). Scale bars = 20 μm.

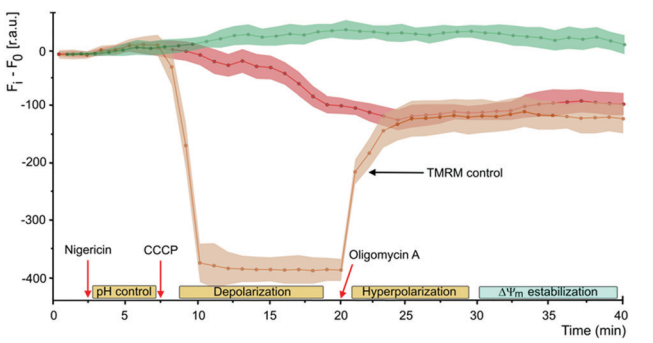

Fig. 4 Induced mitochondrial voltage changes in HeLa cells. Relative fluorescence intensity ($F_i - F_0 \pm$ SEM in r.a.u.) *vs.* time (min) for 1 μM **RVolt** (green and red lines) and TMRM® mitochondrial localizer control (orange line) upon *in situ* additions of 100 nM nigericin, 150 nM CCCP (after 5 min) and 5 μg mL^{-1} oligomycin A at 20 min. SLM-spectrophotometer setup ($\lambda_{exc}/\lambda_{em}$): green (488/510 nm), red (700/715 nm) and orange (605/615 nm). Point recordings were taken by 1 min time-lapse.

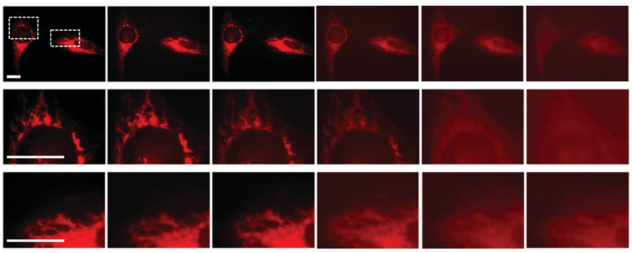

Fig. 5 Effect of mPTP opening detected in the deep-red confocal channel (λ_{exc} = 647 nm) for HeLa cells before (first panel-left) and after 5 min treatment with 400 μM $CaCl_2$ (panels 2–6). The images were taken each 2 minutes and were manually focused, excitation light was fully shielded between recordings to prevent artefacts and photobleaching. Scale bars = 20 μm.

CCCP stimuli, nigericin does not completely inhibited mitochondrial depolarization (the slight fluorescence increments after nigericin treatment in Fig. 4). Interestingly, this subtle effect was successfully monitored by the **RVolt**, fluorescence profiles in the green and red lines of Fig. 4. Then, the elicited responses upon treatment with CCCP and OA were corroborated as expected, red and green profiles in Fig. 4. As can be seen, CCCP increases the rate of PET process in the **RVolt** causing a fluorescence decrease in the red confocal channel and a slight increment (almost constant) of the fluorescence intensity in the green confocal channel. The OA treatment that slows down such electron transfer resulted in the **RVolt** fluorescence activation inside the organelle. Since the mitochondrial membrane potential is only a part of the transmembrane potential energy coming from the proton gradient ($\Delta\mu H^+$) on the inner mitochondrial membrane,[18] regulation of the proton gradient is desirable. In fact, experiments without nigericin treatment produced notorious mitochondrial damage and noisy fluorescence variations just after CCCP treatment.

Finally, we envisioned that a promising strategy to release the hydrolyzed **RVolt** probe from the mitochondrial interior, thus corroborating that the probe is trapped inside the organelle by a non-Nernstian mechanism should involve the opening of the mitochondrial permeability transition pore (mPTP) and not through a diffusion driven by CCCP depolarization. Firstly, we conducted a mass spectrometry **RVolt** titration with esterase (carboxyl ester hydrolase) to assess the hydrolysis reaction occurring from **RVolt** to **Control** probe. Fig. S3 (ESI†) shows that **Control** probe is in fact formed upon esterase additions, corroborating the effectiveness of this hydrolizable function, similar to the Calcein AM protocol (MitoProbe™ Transition Pore Assay Kit).[19] Then, experiments with the mPTP opening resulted in the release of the hydrolyzed **RVolt** probe, Fig. 5. mPTP opening is a non-selective mechanism by which small molecules pass out the mitochondrial membrane, for this reason we envisioned that a control experiment to demonstrate that the hydrolyzed version of the fluorophore is the one being released, would be critical. Treatment with 400 μM $CaCl_2$ was used to selectively induce mPTP opening without causing organelle swelling.[20] Comparison between Fig. 1C (green and red confocal channels) and Fig. 5 indicates that **Control** probe and the *in situ* esterase hydrolyzed **RVolt** probe released by mPTP opening have highly similar imaging patterns, that is, a cytoplasmic localization for both thus suggesting that the **RVolt** can be released by the activation of the mPTP opening process and not by a Nernstian mechanism.

The **RVolt** is a powerful new tool for the monitoring of mitochondrial membrane voltage variations. With a simple electronic dipolar fluorophore as a local polarity reporter, the PET process was successfully correlated with voltage variations and local polarity and under mitochondrial pH control to isolate the fluorescent profiles from factors other than voltage variations. The mPTP opening study is critical to corroborate the non-Nernstian mechanism of voltage probes. The present strategy may find utility in the design and development of new fluorescent probes with slow permeability for multiplexing assays correlating membrane voltage and physicochemical parameters such as local viscosity, polarity and redox status at the subcellular level.

Conflicts of interest

There are no conflicts to declare.

Notes and references

1 A. A. Bazhin, R. Sinisi, U. Marchi, A. Hermant, N. Sambiagio, T. Maric, G. Budin and E. A. Goun, *Nat. Chem. Biol.*, 2020, **16**, 1385.
2 Y. Wang, E. Xu, P. R. Musich and F. Lin, *CNS Neurosci. Ther.*, 2019, **25**, 816.
3 V. A. Popkov, E. Y. Plotnikov, D. N. Silachev, I. B. Pevzner, S. S. Jankauskas, V. A. Babenko, S. D. Zorov, A. V. Balakireva, M. Juhaszova, S. J. Sollott and D. B. Zorov, *Anal. Biochem.*, 2018, **552**, 50.
4 M. Momcilovic, *et al.*, *Nature*, 2019, **575**, 380. See ESI† for the full name list.
5 M. Grabe and G. Oster, *J. Gen. Physiol.*, 2001, **117**, 329.
6 X. Tian, L. C. Murfin, L. Wu, S. E. Lewis and T. D. James, *Chem. Sci.*, 2021, **12**, 3406.
7 D. C. Magri, *Coord. Chem. Rev.*, 2021, **426**, 213598.
8 G. A. Rutter, P. Burnett, R. Rizzuto, M. Brini, M. Murgia, T. Pozzan, J. M. Tavaré and R. M. Denton, *Proc. Natl. Acad. Sci. U. S. A.*, 1996, **93**, 5489.
9 J. J. Lemasters and V. K. Ramshesh, *Methods Cell Biol.*, 2007, **80**, 283.
10 H. Rottenberg and S. Wu, *Biochim. Biophys. Acta*, 1998, **1404**, 393.
11 M. Savarese, C. A. Guido, E. Brémond, I. Ciofini and C. Adamo, *J. Phys. Chem. A*, 2017, **121**, 7543.
12 R. L. Martin, *J. Chem. Phys.*, 2003, **118**, 4775.
13 P. E. Z. Klier, J. G. Martin and E. W. Miller, *J. Am. Chem. Soc.*, 2021, **143**, 4095.
14 R. Flores-Cruz and A. Jiménez-Sánchez, *Chem. Commun.*, 2018, **54**, 13997.
15 S. W. Perry, J. P. Norman, J. Barbieri, E. B. Brown and H. A. Gelbard, *Biotechniques*, 2011, **50**, 98.
16 J. P. Norman, S. W. Perry, K. A. Kasischke, D. J. Volsky and H. A. Gelbard, *J. Immunol.*, 2007, **178**, 869.
17 J. P. Norman, S. W. Perry, H. M. Reynolds and M. Kiebala, *et al.*, *PLoS One*, 2008, **3**(11), e3731.
18 D. Zorova, V. A. Popkov, E. Y. Plotnikov and D. N. Silachev, *et al.*, *Anal. Biochem.*, 2018, **552**, 50.
19 MitoProbe™ Transition Pore Assay Kit (M34153). Molecular probes, 2007. For a representative reference please see: A. J. Kowaltowski, S. S. Smaili, J. T. Russell and G. Fiskum, *Am. J. Physiol.: Cell Physiol.*, 2000, **279**, C852.
20 M. Panel, B. Ghaleb and D. Morin, *Sci. Rep.*, 2017, **7**, 4283.